Journal of Computational Mathematics, Vol.26, No.1, 2008, 23–36.

A PERTURBATION METHOD FOR THE NUMERICAL SOLUTION OF THE BERNOULLI PROBLEM*

François Bouchon
Laboratoire de Mathématiques, Université Blaise Pascal (Clermont-Ferrand) and CNRS (UMR 6620)
Campus Universitaire des Cézeaux, 63177 Aubière cedex, France
Email: Francois.Bouchon@math.univ-bpclermont.fr
Stéphane Clain
Laboratoire MIP, UFR MIG, Université Paul Sabatier Toulouse 3, 118 route de Narbonne, 31062 Toulouse cedex 4, France
Email: clain@mip.ups-tlse.fr
Rachid Touzani
Laboratoire de Mathématiques, Université Blaise Pascal (Clermont-Ferrand) and CNRS (UMR 6620)
Campus Universitaire des Cézeaux, 63177 Aubière cedex, France
Email: Rachid.Touzani@univ-bpclermont.fr

Abstract

We consider the numerical solution of the free boundary Bernoulli problem by employing level set formulations. Using a perturbation technique, we derive a second order method that leads to a fast iteration solver. The iteration procedure is adapted in order to work in the case of topology changes. Various numerical experiments confirm the efficiency of the derived numerical method.

Mathematics subject classification: 35R35, 34E10, 65M06.
Key words: Bernoulli problem, Free boundary, Level sets.

1. Introduction

The Bernoulli problem stands for a prototype of a large class of stationary free boundary problems involved in fluid dynamics and electromagnetic shaping (see [5, 6, 8] and the references therein). This problem roughly consists in a Laplace equation with an additional boundary condition that enables determining the solution of the equation as well as the unknown domain.

In order to obtain a reliable numerical approximation for this problem, a wide variety of works have been produced. For instance, in Flucher and Rumpf [7], some numerical schemes based on a local parametrization are developed. The authors prove in this work convergence results and present some numerical examples. Nevertheless, due to the local parametrization, the constructed methods cannot handle topological changes. In [3], we propose an extension of the Flucher-Rumpf technique introducing a level set formulation to characterize the free boundary. This approach enjoys the property of allowing topology changes as level sets generally do. However, the scheme developed in [3] has the drawback to slowly converge and produces some local oscillation of the computed boundary when the numerical solution approaches the steady state. This drawback is removed in [11] where the authors consider an integral formulation of the Bernoulli problem and where the level set equation is solved via the Fast Marching strategy. The integral representation is however specific to partial differential equations for which this is available.

* Received February 28, 2007 / Revised version received June 4, 2007 / Accepted July 19, 2007 /

In order to improve the solver performances, we propose in this paper a second-order scheme that can be viewed as a Newton-like method. The method is based on a perturbation of the parametrization of the initial guess of the free boundary. It has, as will be shown, the advantage of accelerating the convergence to the steady state solution, but as high-order methods require additional regularity properties, the presented method fails to converge when a topology change occurs during the iteration process. We then resort to switching to the first-order method while a domain splits up or two subdomains collapse. Numerical experiments show that convergence properties are dramatically improved when compared to the algorithm developed in [3].

The outline of the paper is as follows: In Section 2, we present a perturbation method to derive a second-order formulation. Section 3 is devoted to the derivation of a numerical scheme based on level sets and inspired by this perturbation technique. Section 4 presents some numerical results for both a radial case for which the analytical solution is known and a case with changing topology. Finally, a conclusion is drawn.

Let us mention that only the interior Bernoulli problem (see [3] for instance) is considered in the present study. An analog analysis of the exterior problem can be deduced straightforwardly.

2. The Perturbed Problem

Let Ω be a bounded domain of $\mathbb{R}^2$ with a C^2-boundary $\partial\Omega$. We seek a (not necessarily connected) domain A with $\bar{A} \subset \Omega$ and a function u defined on $\Omega \setminus A$ such that:

$$\Delta u = 0 \qquad \text{in } \Omega \setminus \bar{A}, \tag{2.1}$$

$$u = 0 \qquad \text{on } \partial\Omega, \tag{2.2}$$

$$u = 1 \qquad \text{on } \partial A, \tag{2.3}$$

$$\frac{\partial u}{\partial n} = \lambda \qquad \text{on } \partial A, \tag{2.4}$$

where λ is a positive real number and n is the unit normal to the boundary $\partial(\Omega \setminus \bar{A})$ of $\Omega \setminus \bar{A}$ pointing inward A.

We propose, in this section, an alternative to the result obtained in by Flucher and Rumpf (see [7], Theorem 2).

Proposition 2.1. *Let $\partial\tilde{A} = \partial A + \rho n$ be a set close to A (in the sense that $\rho \ll 1$). Then the function u — extended to $\Omega \setminus \tilde{A}$ if necessary — is solution to the following problem:*

$$\Delta u = 0 \qquad \textit{in } \Omega \setminus \bar{\tilde{A}}, \tag{2.5}$$

$$u = 0 \qquad \textit{on } \partial\Omega, \tag{2.6}$$

$$\frac{\partial u}{\partial \tilde{n}} - \tilde{\kappa} u = \lambda - \tilde{\kappa} + \mathcal{O}(\rho^2) \qquad \textit{on } \partial\tilde{A}, \tag{2.7}$$

where $\tilde{\kappa}$ is the curvature of $\partial\tilde{A}$.

To prove this result, we first need to consider some preliminary results.

2.1. Some technical results

Let $\gamma : [0, L] \to \mathbb{R}^2$ denote a parametric representation of the curve ∂A. We choose the parametrization such that the unit normal vector n to ∂A points inward A. The tangent vector

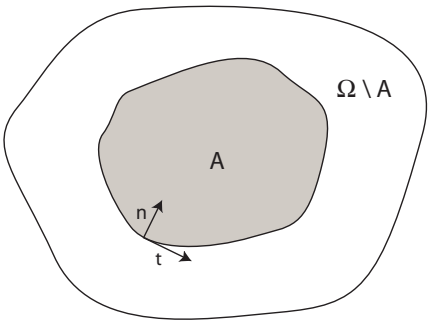

Fig. 2.1. Geometry of the domain.

t is chosen according to Fig. 2.1. We recall that if $\kappa = \kappa(s)$ is the curvature of ∂A at $\gamma(s)$, then we have the Serret-Frénet formulae:

$$\frac{d\gamma}{ds} = t, \quad \frac{dt}{ds} = \kappa\, n, \quad \frac{dn}{ds} = -\kappa\, t.$$

To describe the perturbed boundary $\partial\tilde{A}$ by the parametric function $\tilde{\gamma}(s)$ on $[0, L]$, we assume that there exists a smooth function ρ defined on $[0, L]$ such that

$$\tilde{\gamma}(s) = \gamma(s) + \rho(s)\, n(s) \qquad 0 \le s < L. \tag{2.8}$$

We assume furthermore that

$$\frac{d\rho}{ds} = \mathcal{O}(\rho), \tag{2.9}$$

$$\tilde{\kappa} = \kappa + \mathcal{O}(\rho), \tag{2.10}$$

which means that highly oscillating boundary perturbations are excluded. Let us prove a useful technical result.

Lemma 2.1. *We have the following identities:*

$$\tilde{t} = \frac{1}{D}\Big((1 - \rho\kappa)\, t + \frac{d\rho}{ds}\, n\Big),$$
$$\tilde{n} = \frac{1}{D}\Big((1 - \rho\kappa)\, n - \frac{d\rho}{ds}\, t\Big),$$

with

$$D = \Big((1 - \rho\,\kappa)^2 + \big(\frac{d\rho}{ds}\big)^2\Big)^{\frac{1}{2}}.$$

Proof. The first identity is obtained by differentiation of (2.8) and normalization. The second identity is easily deduced from the first one.

Lemma 2.2. *Let u be a smooth function defined on A and satisfying Eqs.* (2.1)-(2.4)*. Then we have*

$$n^T H(u)\, n = \kappa\, \frac{\partial u}{\partial n},$$

where $H(u)$ is the Hessian matrix of u.

Proof. From equation (2.3), we have $u(\gamma(s)) = 1$. By differentiating, we obtain

$$\nabla u(\gamma(s)) \cdot t(s) = 0.$$

A second differentiation implies

$$t^T H(u(\gamma(s)))\, t + \kappa(s)\, \nabla u(\gamma(s)) \cdot n(s) = 0.$$

From the identity

$$\Delta u = t^T H(u)\, t + n^T H(u)\, n = 0,$$

we get

$$-n^T H(u)\, n + \kappa(s) \nabla u(\gamma(s)) \cdot n(s) = 0.$$

2.2. Proof of Proposition 2.1

For the sake of simplicity, we omit to mention the variable s.

Lemma 2.3. *Let u denote a solution of problem* (2.1)-(2.4)*, admitting a harmonic extension in a neighborhood of ∂A. Then we have*

$$\frac{\partial u}{\partial \tilde{n}} = \lambda + \rho\, \kappa\, \lambda + \mathcal{O}(\rho^2) \qquad \text{on } \partial \tilde{A}. \tag{2.11}$$

Proof. Using Lemma 2.1, we write

$$\frac{\partial u}{\partial \tilde{n}}(\tilde{\gamma}) = \frac{1}{D}\, \nabla u(\gamma + \rho\, n) \cdot \big((1 - \rho\, \kappa)\, n - \frac{d\rho}{ds}\, t\big). \tag{2.12}$$

Differentiating (2.3) in the tangential direction, we get $\nabla u(\gamma) \cdot t = 0$, which gives thanks to the Taylor expansion,

$$\nabla u(\gamma + \rho\, n) \cdot t = \mathcal{O}(\rho). \tag{2.13}$$

Assumption (2.9) implies

$$\begin{aligned} D &= \Big((1 - \rho\, \kappa)^2 + (\frac{d\rho}{ds})^2\Big)^{\frac{1}{2}} \\ &= \Big(1 - 2\rho\, \kappa + \mathcal{O}(\rho^2)\Big)^{\frac{1}{2}} = 1 - \rho\, \kappa + \mathcal{O}(\rho^2), \end{aligned} \tag{2.14}$$

Furthermore, we have by using Lemma (2.2)

$$\begin{aligned} \frac{\partial u}{\partial n}(\gamma + \rho\, n) &= \frac{\partial u}{\partial n}(\gamma) + \rho\, n^T\, H(u(\gamma))\, n + \mathcal{O}(\rho^2) \\ &= (1 + \rho\kappa)\, \frac{\partial u}{\partial n}(\gamma) + \mathcal{O}(\rho^2). \end{aligned} \tag{2.15}$$

Combining (2.13)-(2.15), and Assumption (2.9) again, (2.12) yields

$$\frac{\partial u}{\partial \tilde{n}}(\tilde{\gamma}) = \frac{(1 - \rho\, \kappa)}{D}\, \frac{\partial u}{\partial n}(\gamma + \rho\, n) + \mathcal{O}(\rho^2).$$

We then obtain from Lemma 2.2, and Assumption (2.9)

$$\frac{\partial u}{\partial \tilde{n}}(\tilde{\gamma}) = \frac{1-\rho\kappa}{1-\rho\,\kappa+\mathcal{O}(\rho^2)}\,\frac{\partial u}{\partial n}(\gamma)(1+\rho\,\kappa)+\mathcal{O}(\rho^2)$$
$$= (1+\rho\,\kappa)\,\frac{\partial u}{\partial n}(\gamma)+\mathcal{O}(\rho^2).$$

We conclude by using (2.4).

From Lemma 2.3 and Hypothesis (2.10), we deduce

$$\frac{\partial u}{\partial \tilde{n}}(\tilde{\gamma}) = (1+\rho\tilde{\kappa})\,\lambda+\mathcal{O}(\rho^2).$$

The Taylor expansion

$$u(\tilde{\gamma}) = u(\gamma)+\rho\,\frac{\partial u}{\partial n}(\gamma)+\mathcal{O}(\rho^2) = 1+\rho\,\lambda+\mathcal{O}(\rho^2) \tag{2.16}$$

yields then

$$\frac{\partial u}{\partial \tilde{n}}(\tilde{\gamma}) = \lambda+(u(\tilde{\gamma})-1)\,\tilde{\kappa}+\mathcal{O}(\rho^2).$$

Whence

$$\frac{\partial u}{\partial \tilde{n}}(\tilde{\gamma})-\tilde{\kappa}\,u(\tilde{\gamma}) = \lambda-\tilde{\kappa}+\mathcal{O}(\rho^2).$$

This completes the proof of Proposition 2.1.

Let us now use this material to derive an iterative process to solve problem (2.1)-(2.4): If A_k is a known approximation of the set A, we compute u_k solution of

$$\Delta u_k = 0 \qquad \text{in } \Omega\setminus\bar{A}_k, \tag{2.17}$$
$$u_k = 0 \qquad \text{on } \partial\Omega, \tag{2.18}$$
$$\frac{\partial u_k}{\partial n_k}-\kappa_k u_k = \lambda-\kappa_k \qquad \text{on } \partial A_k, \tag{2.19}$$

where n_k, κ_k are respectively the inward unit normal to ∂A_k and the curvature of ∂A_k. We aim at computing an approximation of ρ such that $\partial A = \partial A_k+\rho n_k$.

Let us set $u' = u_k - u$. Combining (2.5)-(2.7) with (2.17)-(2.19) shows that u' is solution of:

$$\Delta u' = 0 \qquad \text{in } \Omega\setminus\bar{A}_k, \tag{2.20}$$
$$u' = 0 \qquad \text{on } \partial\Omega, \tag{2.21}$$
$$\frac{\partial u'}{\partial n_k}-\kappa_k u' = \mathcal{O}(\rho^2) \qquad \text{on } \partial A_k, \tag{2.22}$$

which shows, at least in the case where $\kappa_k \geq 0$, that $u' = \mathcal{O}(\rho^2)$ on $\Omega\setminus\bar{A}_k$, and then on ∂A_k. Hence $u_k = u+\mathcal{O}(\rho^2)$. From (2.16), we have

$$\rho = \frac{u(\tilde{\gamma})-1}{\lambda}+\mathcal{O}(\rho^2) = \frac{u_k(\tilde{\gamma})-1}{\lambda}+\mathcal{O}(\rho^2).$$

We deduce that the setting

$$A_{k+1} := A_k-\rho_k n_k, \tag{2.23}$$

with

$$\rho_k = \frac{u_k(\tilde{\gamma})-1}{\lambda} \tag{2.24}$$

gives a "good" approximation to A.

In the following section, we present the numerical algorithm in the context of level set methods.

3. Numerical Scheme

Let (A, u) be a smooth solution of the Bernoulli problem (A is C^3 and u is C^2, say). Our aim is to build a sequence $(A_k, u_k)_k$ of solutions of an approximate Bernoulli problem which converges towards (A, u).

We first present the level set method, and then we derive from the previous analysis an iterative scheme which converges provided that the initial guess is not too far from the solution. Finally, we introduce what we will refer to as a mixed scheme.

3.1. The level set formulation

As we emphasized in the previous section, the scheme we have constructed is based on a local description of A_k given by the function ρ_k. If a topology change occurs, such a formulation breaks down and this motivates the introduction of the level set formulation to characterize the free boundary. To obtain a level set formulation, we use the principle that the level set description and the local description with ρ_k must coincide whenever this last one has a sense.

3.1.1. The level set definition

The level set formulation consists in characterizing the boundary of the domain A_k as the zero level set of a function ϕ_k. More precisely, we seek a function ϕ_k such that

$$\begin{aligned} \gamma_k &= \{x \in \Omega;\ \phi_k(x) = 0\}, \\ A_k &= \{x \in \Omega;\ \phi_k(x) > 0\}, \\ \Omega \setminus \bar{A}_k &= \{x \in \Omega;\ \phi_k(x) < 0\}. \end{aligned}$$

Since we state that ϕ_k is positive inside A_k and negative outside, we get that the inward normal vector on ∂A_k is given by

$$n_k = \frac{\nabla \phi_k}{|\nabla \phi_k|}.$$

3.1.2. The level set equation

Let ϕ_k and ϕ_{k+1} be two level set functions associated to the domains A_k and A_{k+1} respectively and assume that we have a local description of the boundary for both A_k and A_{k+1}. By definition, the level set functions satisfy

$$\phi_{k+1}(\gamma_{k+1}) = \phi_k(\gamma_k) = 0, \tag{3.1}$$

and the function γ_{k+1} is given by relation (2.22),

$$\gamma_{k+1} = \gamma_k - \rho_k\, n_{k+1}.$$

The Taylor expansion gives

$$\begin{aligned} \phi_{k+1}(\gamma_{k+1}) &= \phi_{k+1}(\gamma_k - \rho_k n_{k+1}) \\ &= \phi_{k+1}(\gamma_k) - \rho_k\, \nabla \phi_{k+1}(\gamma_k) \cdot n_{k+1} + \mathcal{O}(\rho_k^2). \end{aligned}$$

We can write using identity (3.1),

$$\phi_{k+1}(\gamma_k) = \rho_k\, \nabla \phi_{k+1}(\gamma_k) \cdot n_{k+1} + \mathcal{O}(\rho_k^2).$$

Using the expression of the inward normal

$$\phi_{k+1}(\gamma_k) = \rho_k \nabla\phi_{k+1}(\gamma_k) \cdot \frac{\nabla\phi_{k+1}(\gamma_{k+1})}{|\nabla\phi_{k+1}(\gamma_{k+1})|} + \mathcal{O}(\rho_k^2).$$

Another Taylor expansion shows that

$$\frac{\nabla\phi_{k+1}(\gamma_{k+1})}{|\nabla\phi_{k+1}(\gamma_{k+1})|} = \frac{\nabla\phi_{k+1}(\gamma_k)}{|\nabla\phi_{k+1}(\gamma_k)|} + \mathcal{O}(\rho_k).$$

We finally obtain

$$\phi_{k+1}(\gamma_k) = \rho_k |\nabla\phi_{k+1}(\gamma_k)| + \mathcal{O}(\rho_k^2).$$

Since the domain A_k moves to the domain A_{k+1} thanks to the relation (2.24)

$$\rho_k = \frac{u_k - 1}{\lambda} \quad \text{on } \partial A_k,$$

and recalling that $\phi_k(\gamma_k) = 0$, we obtain the level set equation for the function ϕ_{k+1}

$$\phi_{k+1}(\gamma_k) = \phi_k(\gamma_k) + \frac{u_k - 1}{\lambda} |\nabla\phi_{k+1}(\gamma_k)| + \mathcal{O}(\rho_k^2). \tag{3.2}$$

The function $(1 - u_k)/\lambda$ behaves like a speed of propagation to move the boundary but equation (3.2) is only defined on the domain boundary ∂A_k. To complete the scheme we need an extension of the normal velocity to obtain a level set equation on the whole domain Ω.

3.1.3. Extension of the normal velocity

Following [1], we construct a velocity v_k by the Fast Marching method such that $v_k \cdot n_k$ coincides with the normal velocity $(1 - u_k)/\lambda$ on ∂A_k. To this end, for a given level set function ϕ_k such that $|\nabla\phi_k| = 1$, we solve the equation

$$\nabla v_k \cdot \nabla\phi_k = 0,$$

with the condition

$$v_k = \frac{1 - u_k}{\kappa_k} \qquad \text{on } \partial A_k.$$

We define ϕ_{k+1} by

$$\begin{aligned}\phi_{k+1} &= \phi_k - v_k|\nabla\phi_{k+1}| \\ &= \phi_k - v_k|\nabla\phi_k + \mathcal{O}(\rho_k)| = \phi_k - v_k + \mathcal{O}(\rho_k^2),\end{aligned}$$

where we have used the property $v_k = \mathcal{O}(\rho_k)$. Now, we have by differentiation

$$\nabla\phi_{k+1} = \nabla\phi_k - \nabla v_k + \mathcal{O}(|\nabla\rho_k^2|).$$

Since we have assumed $|\nabla\rho_k| = \mathcal{O}(\rho_k)$, then

$$\begin{aligned}|\nabla\phi_{k+1}|^2 &= \nabla\phi_k \cdot \nabla\phi_{k+1} - \nabla v_k \cdot \nabla\phi_{k+1} + \mathcal{O}(\rho_k^2) \\ &= \nabla\phi_k \cdot (\nabla\phi_k - \nabla v_k) - \nabla v_k \cdot (\nabla\phi_k - \nabla v_k + \mathcal{O}(\rho_k^2)) + \mathcal{O}(\rho_k^2) \\ &= 1 + \mathcal{O}(\rho_k^2).\end{aligned}$$

The function ϕ_{k+1} is then updated in order to satisfy $|\nabla\phi_{k+1}| = 1$ by using a Fast Marching Method. Note that this correction does not modify the position of the free boundary. To initialize the iterative process, we choose ϕ_0 as the signed distance function associated to the initial guess A_0.

We now design two numerical schemes based on the level set formulation.

3.2. The "perturbation-method scheme"

Let us describe now the algorithm deduced from the analysis of the previous section. Assume that we know the domain A_k and a level set function ϕ_k associated to A_k satisfying $|\nabla\phi_k| = 1$.

(1) We compute u_k on $\Omega \setminus \bar{A}_k$ solving the elliptic problem with mixed condition on the boundary

$$\begin{aligned} &\Delta u_k = 0 && \text{in } \Omega \setminus \bar{A}_k, \\ &u_k = 0 && \text{on } \partial\Omega, \\ &\frac{\partial u_k}{\partial n_k} - \kappa_k u_k = \lambda - \kappa_k && \text{on } \partial A_k, \end{aligned} \tag{3.3}$$

where

$$\kappa_k(x) = \nabla \cdot \Big(\frac{\nabla\phi_k(x)}{|\nabla\phi_k(x)|}\Big).$$

(2) We compute the extended normal velocity v_k on Ω by

$$\begin{aligned} &\nabla v_k \cdot \nabla\phi_k = 0 && \text{in } \Omega, \\ &v_k = \frac{1 - u_k}{\lambda} && \text{on } \partial A_k, \end{aligned}$$

using the Fast Marching method described in [1].

(3) We obtain the new level set function ϕ_{k+1} by setting

$$\phi^*_{k+1}(x) = \phi_k(x) - v_k(x),$$

which defines $\partial A_{k+1} = \{x \in \Omega;\ \phi^*_{k+1}(x) > 0\}$.

(4) We perform a correction step to compute ϕ_{k+1}:

$$\begin{aligned} &|\nabla\phi_{k+1}| = 1 && \text{in } \Omega, \\ &\phi_{k+1} = 0 && \text{on } \partial A_k, \\ &\phi_{k+1}\phi^*_{k+1} \geq 0 && \text{in } \Omega. \end{aligned} \tag{3.4}$$

Note that the last equation imposes that the sign of ϕ_{k+1} remains the same as the sign of ϕ^*_{k+1}. This step is performed using again the Fast Marching method ([1]).

3.3. The Neumann scheme

Since the previous scheme converges locally (if the initial guess is close enough to the solution A), our aim is to improve it in order to extend its domain of convergence. For this end, we use a scheme close to the Neumann scheme described in [3]: Let A_k be given and ϕ_k be a level set function associated to A_k. We consider the following algorithm.

(1) We compute u_k on $\Omega \setminus \bar{A}_k$ by solving the elliptic problem

$$\begin{aligned} &\Delta u_k = 0 && \text{in } \Omega \setminus \bar{A}_k, \\ &u_k = 0 && \text{on } \partial\Omega, \\ &\frac{\partial u_k}{\partial n_k} = \lambda && \text{on } \partial A_k. \end{aligned}$$

(2) We compute the extended normal velocity v_k on Ω by

$$\begin{aligned} \nabla v_k \cdot \nabla \phi_k &= 0 && \text{in } \Omega, \\ v_k &= \frac{1-u_k}{\lambda} && \text{on } \partial A_k, \end{aligned}$$

using the Fast Marching method described in [1].

(3) We obtain the new level set function ϕ_{k+1} by setting

$$\phi^*_{k+1}(x) = \phi_k(x) - v_k(x),$$

which defines $\partial A_{k+1} = \{x \in \Omega;\ \phi^*_{k+1}(x) > 0\}$.

The correction step (3.4) enables computing ϕ_{k+1}.

The main advantage of this scheme is that we do not have to introduce the curvature. Its drawback resides in its limitation to the context of elliptic solutions (see [7] and [3] for further details).

3.4. The mixed scheme

As many "Newton-like" schemes, the perturbation-method scheme experiences a high rate of convergence provided the initial guess is close enough to the solution. If the starting point is too far (for example, if a topology change is necessary to reach the solution), then the Neumann scheme shall be used.

Since the curvature of the set exhibits some singularity when facing a topology change, we have chosen as criterion the maximum value of the curvature to determine which scheme to use. Namely, at each iteration k, if the maximum value of the curvature κ_k is too large, then we choose the second scheme ("Neumann Scheme") and if it is small enough, then we choose the "perturbation-method scheme". In practice, the chosen criterion is given by

$$\frac{1}{\kappa} \leq Ch$$

where h is the grid size and C is a given constant that ensures convergence of the numerical scheme (see [4]).

4. Numerical Results

In order to solve the numerical problem, we resort to the classical five-point finite difference scheme for the Laplace equation. We have implemented the obtained discrete problem in four configurations. The first one aims to evaluate the convergence rate of the scheme. The second one aims at showing that the scheme can converge in the both cases of elliptic and hyperbolic solutions (depending on the initial guess). The notion of hyperbolic solution is the one defined in [7].

In the two last configurations, we observe topology changes.

4.1. Convergence tests

In this series of tests we consider first the adaptation of the described scheme to the exterior Bernoulli problem. We next consider an interior Bernoulli problem.

We have chosen $\Omega = \{x \in \mathbb{R}^2; |x - c| < \rho_0\}, \rho_0 = 0.2, c = (0.5, 0.5)$. In this case, the only solution is the circle centered in c of radius ρ such that

$$\lambda = \frac{1}{\rho\,(\log\rho - \log\rho_0)}.$$

We have chosen $\lambda = 7$, for which the solution is the circle of radius $\rho_1 \approx 0.3148\cdots$.

Table 4.1 shows the Hausdorff distance to this solution (denoted by A_∞) when we take as initial guess the circle centered in c of radius 0.30. Recall that the Hausdorff distance is defined by (see [3])

$$D(A, B) := \max\left(\sup_{a\in A}(a, B), \sup_{b\in B}(b, A)\right) \quad A, B \subset \mathbb{R}^2,$$

where $d(a, B) := \inf_{b\in B}|a - b|$. To calculate this distance we use the signed distance function ϕ_k.

The stop criterion has been defined using the Hausdorff distance between two consecutive sets A_k, A_{k+1}. Since we expect a second order scheme, the stop criterion must be finer than the grid size h^2. In our numerical tests, we have fixed the criterion

$$D(A_{k_{f-1}}, A_{k_f}) < h^3.$$

Note that an erratic convergence behavior is observed for a coarse grid.

Table 4.1 also shows that the CPU time increases significantly within the grid size. This is natural since each iteration requires the solution of the elliptic problem (3.3) with an increasing number of unknowns.

Table 4.1: Convergence test for the elliptic solution.

Grid	$D(A_k, A_\infty)$	Rate	Nb. Iter.	Time *(sec.)*
40×40	4.17×10^{-4}		12	30.6
60×60	1.73×10^{-4}	2.2	13	52.4
80×80	1.63×10^{-4}	0.2	4	23.7
120×120	6.10×10^{-5}	2.4	5	49.2
160×160	3.50×10^{-5}	1.9	5	80.0
240×240	1.82×10^{-5}	1.6	5	190.8
320×320	9.47×10^{-6}	2.3	6	510.5
480×480	4.39×10^{-6}	1.9	6	2711.9
640×640	2.43×10^{-6}	2.0	6	5743.4

We observe the convergence history for two particular grid sizes: 60×60 (solid line) and 80×80 (dotted line). The condition linking the curvature and the grid size is satisfied in this the test for the grid 80×80, the algorithm converges then faster. For the 60×60 grid, the mesh size $h = 1/60$ is too coarse and the first algorithm is used, this is the reason why we need more iterations to reach convergence. Table 4.1 shows a second-order convergence rate behavior.

To consider an interior Bernoulli problem example, we choose $\Omega = \{x \in \mathbb{R}^2; |x - c| < \rho_0\}, \rho_0 = 0.42, c = (0.5, 0.5)$. In this case, any circle centered in c of radius ρ such that

$$\lambda = \frac{1}{\rho\,(\log\rho - \log\rho_0)}$$

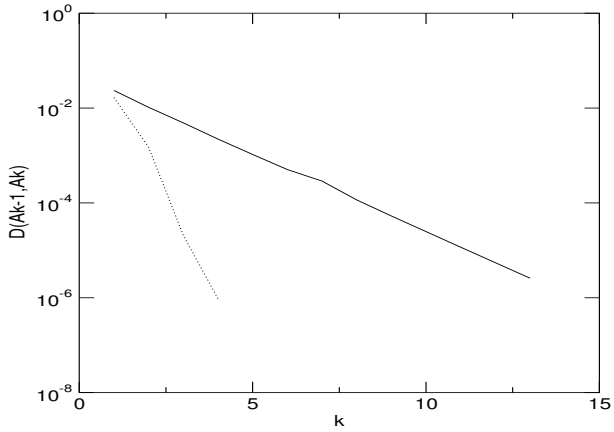

Fig. 4.1. Convergence history for the 60×60 grid (solid line) and 80×80 grid (dotted line).

is a solution of the problem. We have chosen $\lambda = 7$, the circle of radius $\rho_1 \approx 0.218285\cdots$ is the elliptic solution, and the circle of radius $\rho_2 \approx 0.098528\cdots$ is the hyperbolic solution.

Table 4.2: Convergence test for the elliptic solution.

Grid	$D(A_k, A_\infty)$	Rate	Nb. Iter.	Time *(sec.)*
40×40	1.63×10^{-3}		17	45
60×60	1.01×10^{-3}	1.2	19	73
80×80	7.63×10^{-4}	1.0	23	127
120×120	1.61×10^{-4}	3.8	7	82
160×160	1.04×10^{-4}	1.5	7	160
240×240	5.77×10^{-5}	1.4	7	581
320×320	3.36×10^{-5}	1.9	7	2253
480×480	1.33×10^{-5}	2.3	8	17167
640×640	7.73×10^{-6}	1.9	8	51783

Table 4.3: Convergence test for the hyperbolic solution.

Grid	$D(A_k, A_\infty)$	Rate	Nb. Iter.	Time *(sec.)*
40×40		*(no convergence)*		
60×60		*(no convergence)*		
80×80		*(no convergence)*		
120×120		*(no convergence)*		
160×160		*(no convergence)*		
240×240	1.02×10^{-4}		6	626
320×320	4.99×10^{-5}	2.5	6	2262
480×480	4.01×10^{-5}	0.5	5	19397
640×640	1.38×10^{-5}	3.7	5	59394

Table 4.2 shows the Hausdorff distance to the solution when we take as initial guess the circle centered in c of radius 0.32. Note that, in this case, the algorithm converges to the elliptic solution (which has been taken as reference solution A_∞). Here also, a second-order convergence rate is observed.

Table 4.3 shows the Hausdorff distance to the solution when we take as initial guess the circle

centered in c of radius 0.1. Note that, in this case, the algorithm converges to the hyperbolic solution (which has been taken as reference solution A_∞). No convergence rate can however be deduced from numerical experiments.

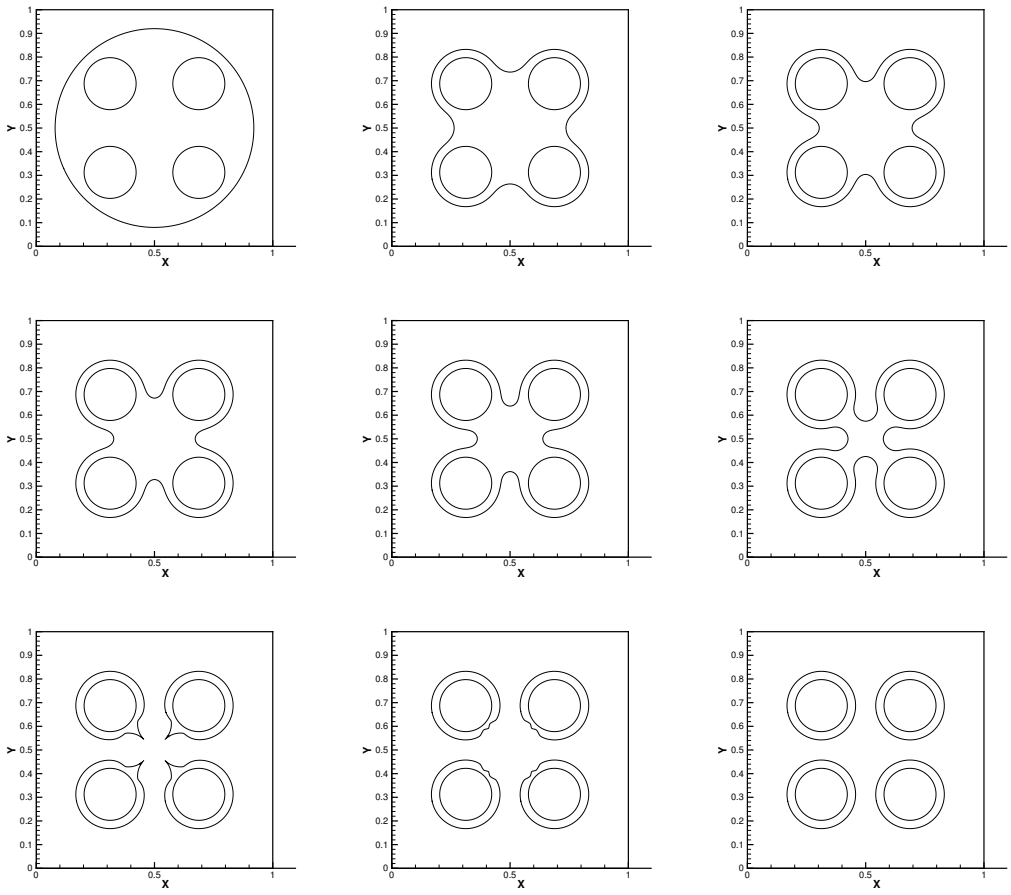

Fig. 4.2. Domains A_0 to A_{30}.

For the coarse grids, the criterion on the curvature is not satisfied. Then, the first (Neumann) scheme is used, and since it works only in the elliptic context, then we have no convergence of our algorithm (namely, the set A_k is empty for some k).

4.2. Topology change tests

In this test, Ω is the union of four disks of radius 0.11 centered at $P_1 = (0.3125, 0.3125)$, $P_2 = (0.6875, 0.3125)$, $P_3 = (0.3125, 0.6875)$ and $P_4 = (0.6875, 0.6875)$ respectively. The value of λ has been taken equal to 25, and the initial guess is a disk centered at $(0.5, 0.5)$ of radius 0.42 (containing Ω). The exact solution is given by the union of four disjointed disks centered at P_1, P_2, P_3 and P_4.

We have run this test on a 240×240 grid, with an initial guess consisting in a disk containing $\bar{\Omega}$. Convergence has been reached after 32 iterations (1272 sec.).

Fig. 4.2 shows the evolution of the boundary A_0, A_5, A_{10}, A_{15}, A_{20}, A_{23}, A_{24}, A_{25} and A_{30}.

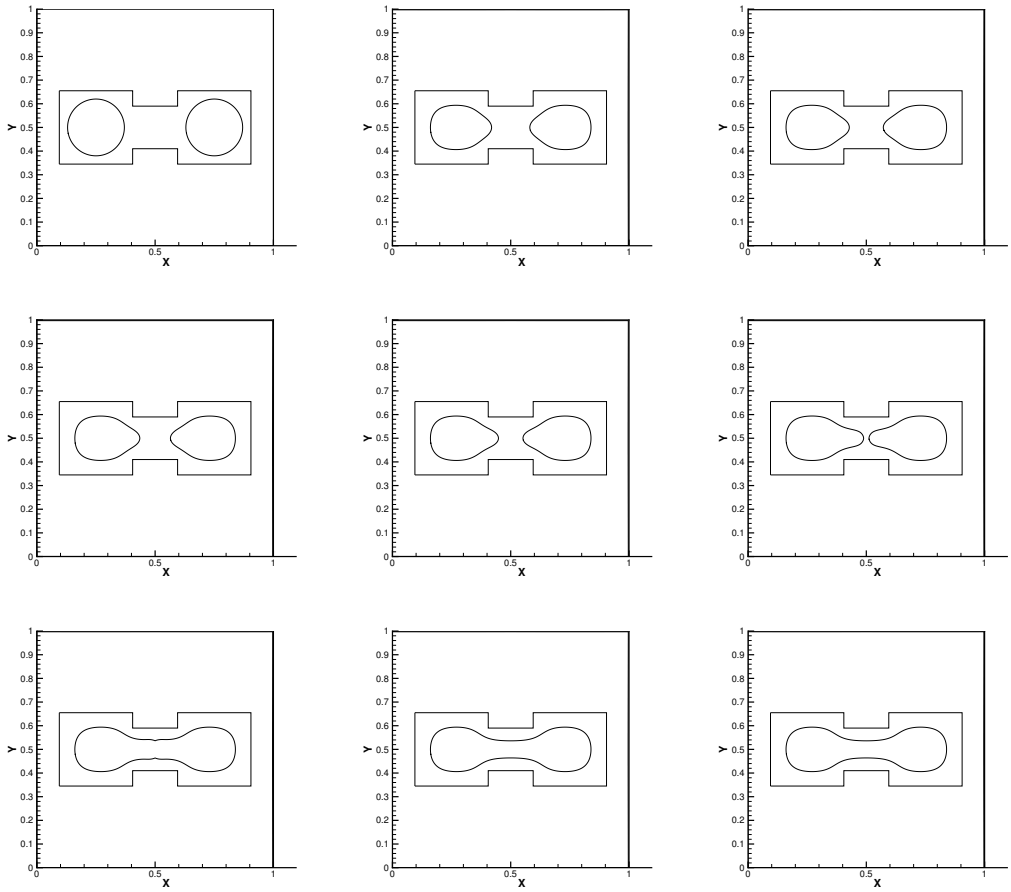

Fig. 4.3. Domains A_0 to A_{55}.

To consider an interior topology change test, Ω is a set similar to the set used by Flucher and Rumpf [7]. λ has been taken equal to -18, and the initial guess is the union of two disks centered at $(0.25, 0.5)$ and $(0.75, 0.5)$ of radius 0.12 *(included in Ω)*.

We have run this test on a 240×240 grid; convergence has been reached after 55 iterations (1374.1 sec).

Fig. 4.3 shows the evolution of the boundary A_0, A_{10}, A_{20}, A_{30}, A_{40}, A_{46}, A_{47}, A_{50} and A_{55}.

5. Conclusion

In this paper we have presented various extensions of the Flucher and Rumpf numerical method to allow topological change. The method is based on a level set formulation coupled with an elliptic equation derived by asymptotic analysis. Two schemes have been proposed: The first one is devoted to the computation of an accurate solution but requires regularity and does not allow topological changes. The second one is designed to overcome this difficulty but is less accurate. A hybrid technique based on both schemes yields a good convergence speed and a robust solver for the Bernoulli problem.

References

[1] D. Adalsteinsson and J. A. Sethian, The fast construction of extension velocities in level set methods, *J. Comput. Phys.*, **148** (1999), 2-22.

[2] A. Beurling, On free-boundary problems for the Laplace equation, sem. on analytic function, *Inst. Adv. Stud. Princeton,* **1** (1957), 248-263.

[3] F. Bouchon, S. Clain and R. Touzani, Numerical solution of the free boundary Bernoulli problem using a level set formulation, *Comput. Methods Appl. Mech. Eng.*, **194**:36-38 (2005), 3934-3948.

[4] F. Bouchon and G. Peichl, A second order immersed interface technique for an elliptic neumann problem, *Numer. Meth. Part. Diff. Eq.*, **23** (2007), 400-420.

[5] M. Crouzeix, Variational approach of a magnetic shaping problem, *Eur. J. Mech. B-Fluid.,* **10** (1991), 527-536.

[6] J. Descloux, Stability of the solutions of the bidimensional magnetic shaping problem in absence of surface tension, *Eur. J. Mech. B-Fluid.,* **10** (1991), 513-526.

[7] M. Flucher and M. Rumpf, Bernoulli's free-boundary problem, Qualitative theory and numerical approximation, *J. Reine Angew. Math.*, **486** (1997), 165-204.

[8] A. Friedman, Free boundary problem in fluid dynamics, Société Mathématique de France, Astérisque, **118** (1984), 55-67.

[9] J. Haslinger, T. Kozubek, K. Kunisch and G. Peichl, Shape optimization and ficticious domain approach for solving free-boundary problems of Bernoulli type, *Comput. Optim. Appl.*, **26** (2003), 231-251.

[10] K. Ito, K. Kunisch and G.H. Peichl, Variational approach to shape derivatives for a class of Bernoulli problems, *J. Math. Anal. Appl.*, **314** (2006), 126-149.

[11] C.M. Kuster, P. Gremaud, R. Touzani, Fast numerical methods for Bernoulli free boundary problems, *SIAM J. Sci. Comput.*, to appear.

[12] K. Kärkkäinen and T. Tiihonen, Free surfaces: shape sensitivity analysis and numerical methods, *Int. J. Numer. Meth. Eng.*, **44** (1999), 1079-1098.

[13] G. Mejak, Numerical solution of Bernoulli-type free boundary value problems by variable domain method, *Int. J. Numer. Meth. Eng.,* **37** (1994), 4219-4245.